

# Nanoparticle based inorganic coatings for corrosion protection of magnesium alloys

F. Feil\*, W. Fürbeth and M. Schütze

Inorganic nanoparticle based coatings for magnesium alloys were developed and tested for their performance in corrosion protection. Nanoparticles are characterised by a high sintering activity. This allows to obtain inorganic coatings by a sintering process at rather low temperatures which is suitable for magnesium alloys. Coating sols are based on silicon dioxide and sintering additives such as boron or sodium oxide. One technique is based on aqueous, commercial nanosols which can be applied by dip or brush coating to form layers on AZ31 and AZ91. Another technique is based on the electrophoretic deposition of silicon dioxide nanoparticles which also contain boron and phosphorus oxide. Crack free layers with a thickness of up to several micrometres could be obtained by a two step process including a bimodal particle distribution and polydiethoxysiloxane as adhesion promoter. The composition and surface structure of these novel coatings are characterised by modern analytical methods including SEM and atomic force microscopy and their applicability as protective coatings is investigated by using electrochemical impedance spectroscopy.

**Keywords:** Corrosion protection, Magnesium alloys, Sol-gel, Electrophoretic deposition, Nanoparticles

## Introduction

Magnesium alloys are increasingly used nowadays in a lot of applications where a reduction of weight without a loss in stability is required. However, due to their high reactivity these alloys require a good protection against corrosion. Established coating methods, e.g. chromating, may not be used anymore due to environmental regulations or are not sufficiently stable under mechanical or thermal influence (e.g. organic coatings).

Besides good corrosion protection dense inorganic coatings may offer also high thermal and mechanical stability. However, mostly the melting point of inorganic coating materials is much higher than the thermal stability of the substrate. Especially magnesium alloys are not stable beyond 200–400°C, depending on the alloy type. Hence the application of inorganic coatings is not possible by conventional methods.

The sintering activity usually increases with decreasing particle size.<sup>1</sup> Owing to the increasing surface per weight ratio of nanoparticles their surface dependent reactions become kinetically more and more important. Therefore, bodies made of nanoparticles densify and combine to firm compounds at rather low temperatures. This allows to use them for the production of glass-like inorganic coatings by a thermal process even suitable for the application on light metals.<sup>2</sup> Appropriate additives, forming eutectic mixtures with silicon dioxide, e.g.

boron oxide or phosphorous oxide, may lower the necessary sintering temperature even further and increase the chemical stability of the coatings.

In the present work purely inorganic and environmentally compliant coatings have been applied to the widespread magnesium alloys AZ31 (wrought alloy) and AZ91 (cast alloy) by coating, brushing and electrophoretic deposition techniques. These coatings are based on commercially available SiO<sub>2</sub> nanopowders and dispersions with suitable additives as well as on nanoparticles composed of silicon, phosphorus and boron oxide made by the sol-gel process.

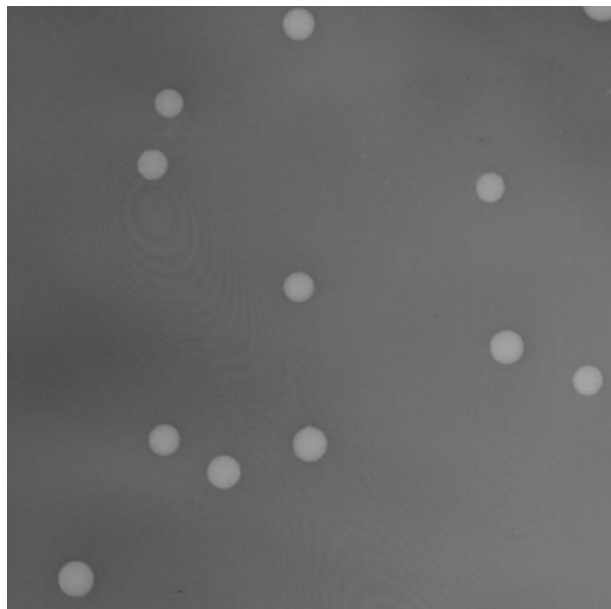
## Experimental

All chemicals and dispersions used have been obtained in the usual qualities (mainly p.a.) from the known suppliers (Sigma-Aldrich, Riedel, Fluka, Bayer, Evonik Degussa, etc.) and have been used without further purification. Aqueous coating sols used are prepared from commercial dispersions and H<sub>3</sub>BO<sub>3</sub>, Na<sub>2</sub>B<sub>4</sub>O<sub>7</sub>, NaH<sub>2</sub>PO<sub>4</sub>, Na<sub>2</sub>HPO<sub>4</sub>, NaOH, KOH, LiOH and Al(OH)<sub>3</sub> dissolved in distilled water. If necessary the pH value can be adjusted to 8–9 with nitric acid. The composition and solid content of the dispersions is listed in Table 1. Mixed silicon, phosphorus and boron oxide nanoparticles for electrophoretic deposition are prepared from tetraethoxysilane (TEOS), triethylborate and triethylphosphate from ethanol and ammonium hydroxide as catalyst.

The substrates to be coated were first of all ground (SiC paper from P1200 to P4000) and degreased in caustic and acetone. For AZ31 a further acidic

Karl-Winnacker-Institut der DECHEMA e.V., Theodor-Heuss-Allee 25, D-60486 Frankfurt am Main, Germany

\*Corresponding author, email feil@dechema.de



**1 Image (TEM) of monodisperse non-agglomerated oxide particles, 200 nm (85.2%SiO<sub>2</sub>, 10.1%B<sub>2</sub>O<sub>3</sub>, 4.7%P<sub>2</sub>O<sub>5</sub>)**

activation with Nital (2% HNO<sub>3</sub> in ethyl alcohol, 5 s) resulted in the best wetting behaviour by water based solutions. AZ91 could best be prepared by a treatment with 2% HNO<sub>3</sub> in glycol/H<sub>2</sub>O (75:25).

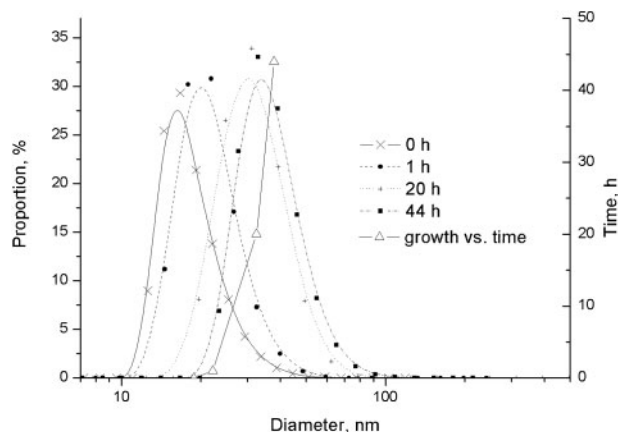
For coating application these prepared samples were either dipped into the coating sol and withdrawn at constant speed (1 cm min<sup>-1</sup>) or whisked in one draw with a brush wetted in the coating sol. Because of possible water electrolysis the EPD was performed from ethanol based dispersions. However, up to 10% water content can be tolerated to increase dispersion stability and conductivity. As an electrolyte and stabiliser ammonia has been used. At pH 9–10 SiO<sub>2</sub> particles are negatively charged. The magnesium sample to be coated was therefore switched as the anode. At a solid content of 2% or less and a constant voltage of up to 5 V coating deposition was performed in up to 30 min.

All samples were dried at room temperature and afterwards sintered in synthetic air (heating rate: 5 K min<sup>-1</sup>, holding time: 2 h)

## Results and discussion

### Coating sols

By a base catalysed sol-gel process (e.g. with NH<sub>3</sub>) starting from alkoxides (e.g. tetraethoxysilane, triethylborate, triethylphosphate) a particulate sol of mostly monodisperse spherical oxide nanoparticles can be formed (Fig. 1).<sup>2,3</sup> The particle size can be customised



**2 Particle size distribution in dispersion of 20 nm particles, borax, Na<sub>2</sub>HPO<sub>4</sub> in H<sub>2</sub>O as function of time; composition: D3 (dynamic light scattering, measurements in highly diluted dispersions)**

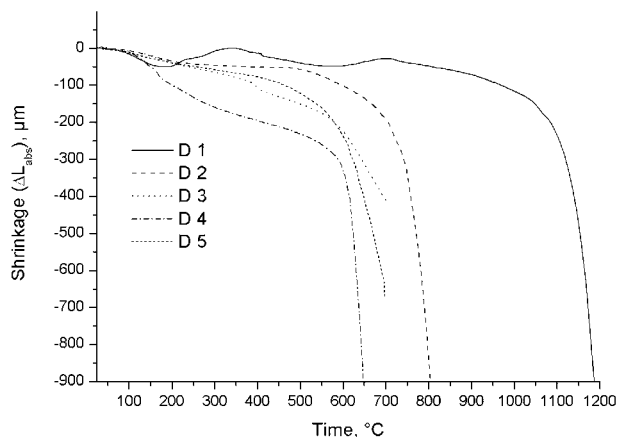
by the reaction conditions (concentration, pH, solvent, water content, etc.) from some nanometres up to micrometres. The electrochemical double layer thereby avoids aggregation of the particles, however, if the solid content in the sol becomes too high agglomeration or early gel formation may occur. Particulate sols may be used directly for coating formation. Higher solid contents are possible by redispersion of centrifugally isolated nanoparticles together with suitable stabilisers (e.g. NH<sub>3</sub>).

Alternatively the coating sol may also be produced based on commercially available silicon dioxide nanoparticles or water based SiO<sub>2</sub> dispersions (e.g. Ludox, Aerodisp, Levasil, etc.). Such particles are available nowadays with a size varying from some nanometres up to micrometres and a narrow size distribution. However, the sintering activity of pure SiO<sub>2</sub> nanoparticles is not high enough to allow moderate coating treatment temperatures. Therefore additional sintering additives in the form of soluble salts (e.g. Na<sub>2</sub>B<sub>4</sub>O<sub>7</sub>, Al(OH)<sub>3</sub>) have to be used.

In coating sols based on commercial SiO<sub>2</sub> dispersions particles react with the sintering additives and agglomerate (Fig. 2). Depending on composition such sols are forming a homogeneous inorganic gel in some minutes or days. Homogeneous gel formation is observed especially with sols containing B<sub>2</sub>O<sub>3</sub>, P<sub>2</sub>O<sub>5</sub> or Al<sub>2</sub>O<sub>3</sub>. Formation of e.g. Si–O–B bonds could be proven by infrared spectroscopy ( $\nu=670\text{ cm}^{-1}$ ).<sup>4,7</sup> Dilatometric measurements of different gel bodies prove that with decreasing particle size also the sintering temperature decreases (Fig. 3). While the melting point of quartz is 1713°C, a body consisting of 20 nm SiO<sub>2</sub> particles

**Table 1 Composition of aqueous dispersions**

Dispersion no.	Particle diameter, nm	Composition of the solid content, wt-%							
		SiO <sub>2</sub>	B <sub>2</sub> O <sub>3</sub>	P <sub>2</sub> O <sub>5</sub>	Al <sub>2</sub> O <sub>3</sub>	Na <sub>2</sub> O	K <sub>2</sub> O	Li <sub>2</sub> O	Solid content, g L <sup>-1</sup>
D1	20	100.0	–	–	–	–	–	–	125
D2	100	88.0	8.3	2.0	–	1.7	–	–	113
D3	20	86.1	6.7	1.8	–	5.4	–	–	112
D4	20	88.5	–	–	2.2	0.9	8.4	–	132
D5	100	83.3	6.9	2.0	–	3.1	2.7	2.0	115
D6	20	76.3	12.8	2.7	0.8	3.3	2.2	1.8	114



**3 Dilatometric measurements (absolute shrinkage versus temperature) of gel bodies consisting of 20 or 100 nm SiO<sub>2</sub> particles (D1–D5)**

densifies already at 1100 $^{\circ}\text{C}$ . Appropriate additives, especially boron, alkali or aluminum oxides, help to decrease the sintering temperature to even lower temperatures. Remarkable is that the presence of small amounts of aluminium helps to start the densification process already at 200 $^{\circ}\text{C}$ .

**Dip and brush coatings**

The coating sol may be applied to the cleaned and activated substrate by dipping or brushing. For dipping the coating thickness is dependent on the viscosity of the sol as well as on the speed of withdrawing the sample from the sol. If pulled out slowly, coatings will be very thin.<sup>8</sup> As magnesium alloys are not stable under acidic conditions sol stabilisation at low pH is not possible.

After drying of particulate sols homogeneous but highly porous gel layers are obtained. The porosity increases with the mean particle size.<sup>8–10</sup> In order to obtain high density of the green layer the solid content of the sol should be as high as possible. However, with increasing solid content also the viscosity of the sol increases leading to a worse wetting behaviour as well as thicker coatings.

Because shrinkage of the coatings during drying and densification is limited to only one dimension the maximum coating thickness is strongly limited. For pure inorganic SiO<sub>2</sub> films the critical thickness without

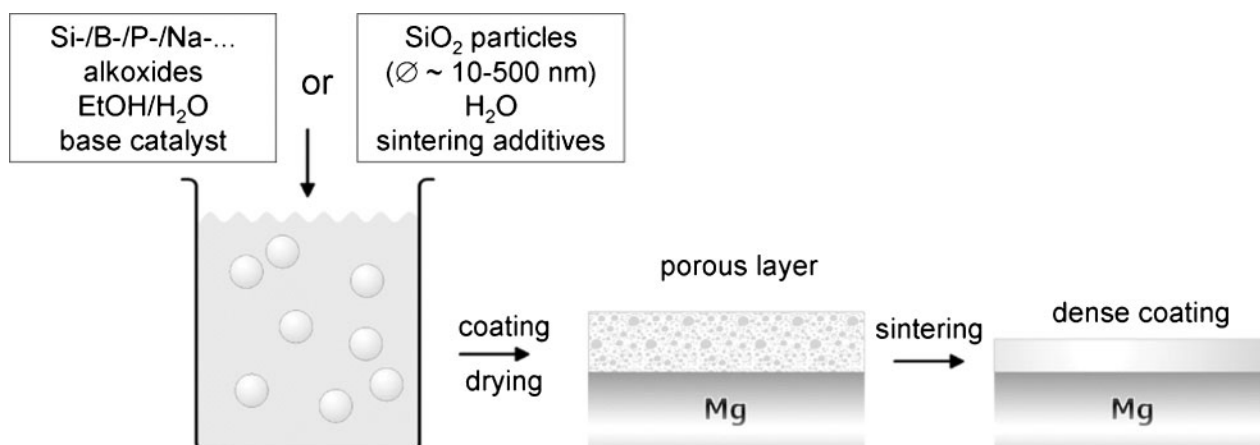
cracking is mostly below 1  $\mu\text{m}$ . Further complicating is the great difference of the thermal expansion coefficients between magnesium ( $26 \times 10^{-6} \text{ K}^{-1}$ ) and the silicate layer (quartz glasses:  $0.55 \times 10^{-6} \text{ K}^{-1}$ , window glasses:  $7.6 \times 10^{-6} \text{ K}^{-1}$ ). This leads to additional stresses during sintering and therefore to cracking or delamination. Nanoparticles may, however, increase the critical coating thickness.<sup>11,12</sup> Suitable additives can be used to adjust the thermal expansion coefficient of the coating to the substrate and this way to avoid cracking. A further possibility to decrease the stresses in the cross-linked coating and to make them more flexible is the use of network modifiers.<sup>9</sup> The whole coating process is schematically shown in Fig. 4.

Dip coated layers tend to become thicker than brushed coatings under the same conditions and therefore have a higher tendency to form cracks within the layer (Fig. 5a). However, with both methods it is possible to obtain thin, crack free layers with a thickness below 1  $\mu\text{m}$  (Fig. 5b).

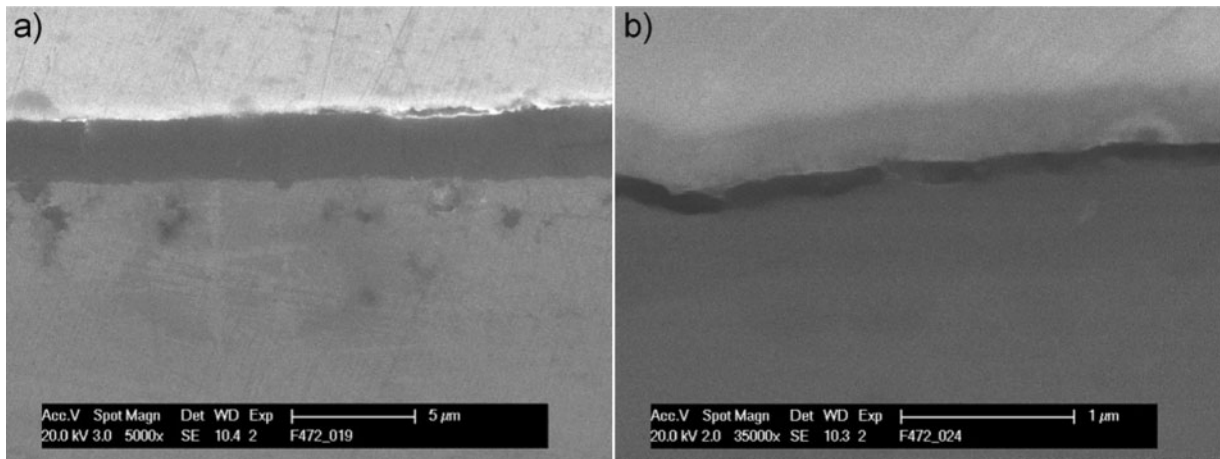
**Electrochemical impedance spectroscopy**

After 30 min immersion in 0.05M Na<sub>2</sub>SO<sub>4</sub> solutions some coated samples show an almost threefold increase of the polarisation resistance compared to the unprotected alloys, as measured by electrochemical impedance spectroscopy (EIS). In particular dip coated layers show rise of the polarisation resistance (Fig. 6), probably because they tend to become thicker than brush coated ones. The protective properties are also dependent on the coating composition.

It can be noted that the difference in the polarisation resistance is relatively small whether an aluminium containing coating is treated at 200 or 400 $^{\circ}\text{C}$ . Neither at 200 nor at 400 $^{\circ}\text{C}$  could the sintering point of the coating materials be achieved, whereas aluminium containing coatings already partially densify at moderate temperatures (Fig. 3: D4), but no complete densification of the coating took place. These porous materials do not isolate the substrate sufficiently. To improve the protective properties either the coating density or the coating thickness has to be increased. Because of the relatively low protective properties of the coatings, circuit diagrams and qualitative statements can not be indicated here but should be developed in further investigations.



**4 Schematic drawing of coating process with particulate sols on magnesium alloys**



a dip coating; b brush coating

##### 5 Images (SEM) from cross-sections of coatings on AZ31 based on D3 sintered at 400°C

### Electrophoretic deposition

An alternative route of coating application is the use of electrophoretic deposition (EPD). This method is based on the fact that in dispersions under an applied electric field, particles will move towards the oppositely charged electrode and will coagulate there. By this method coatings with high green density may be obtained also from dispersions with low solid content. However, only solids will be deposited. Therefore all sintering additives must be contained in the particles. The obtained coating thickness is dependent on concentration, time, voltage and applied current. A further advantage of EPD is that coatings may also be applied to surfaces with complex geometries.<sup>14–17</sup>

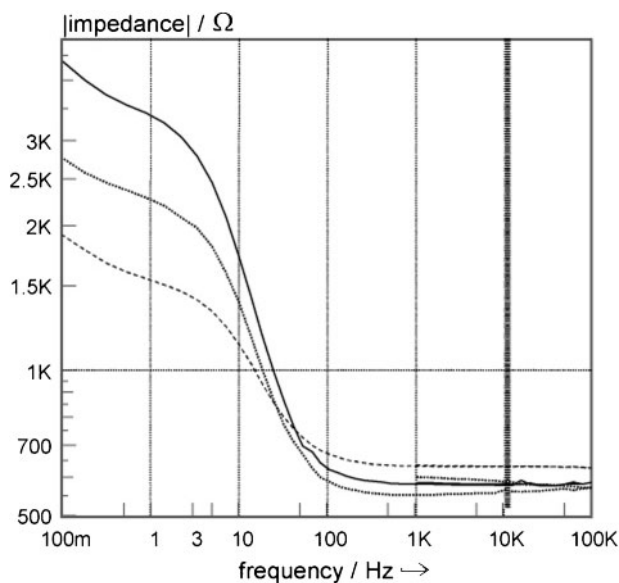
Electrophoretic deposition has been performed with silicon dioxide based particles which also contain boron and phosphorus oxide made by the sol-gel process. For this purpose particulate sols were directly used, or isolated oxide particles were redispersed. Especially at

the beginning of the deposition process a strong decrease in the current can be observed. This shows that the anode surface is covered by isolating nanoparticles. The amount of particles deposited per time decreases with the current flowing. Longer deposition times do not lead to a significantly higher coating thickness.

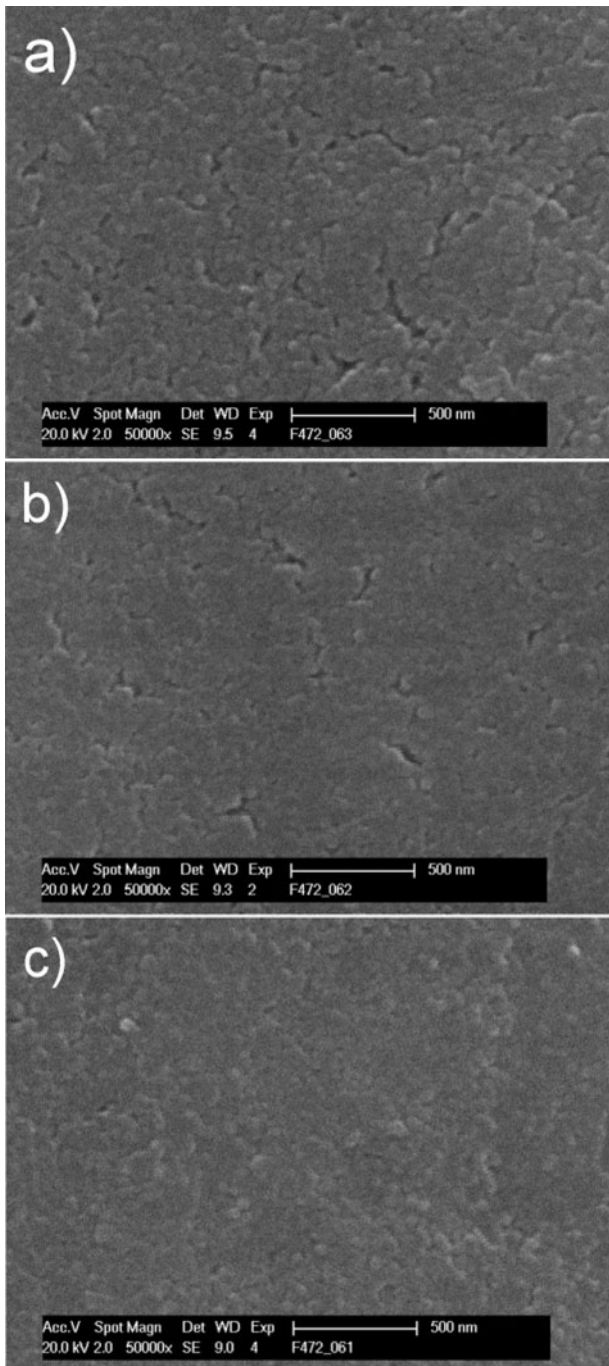
The particle size is very decisive for the maximum obtainable coating thickness by EPD. Small particles (<20 nm) will completely cover the surface much faster so that at very low thicknesses (<100 nm) the current strongly decreases and no further deposition takes place. Larger particles (>200 nm) will lead to thicker coatings of up to 6 μm. However, despite the high green density possible with this method, thicker coatings also tend to form cracks. After sintering crack free coatings could only be obtained below 2 μm so far.

Polydiethoxysiloxane (PDES) can act as adhesion promoter and also help to reduce the tendency to form cracks.<sup>2</sup> Electrophoretic deposition coatings without further additives consisting of 35 nm particles show some microcracks and an average roughness of 15.5 nm after the sintering process (Fig. 7a, roughness is determined by AFM). With the addition of 1 wt-% PDES EPD of these particles results in less cracked layers with an average roughness of 12.7 nm (Fig. 7b). Higher concentrations of PDES do not improve the surface properties, instead an inhibition of the particle deposition can be observed. Particles with boron rich surface can easily be obtained by a modified base catalysed sol-gel process, where the addition of triethylborate is temporarily delayed to the other alkoxides without changing the total composition. Because mainly the particles surface is responsible for the sintering behaviour, these particles show a higher sintering activity. With the addition of 0.5 wt-% PDES their deposition results in crack free coatings with an average roughness of only 5.6 nm (Fig. 7c).

Thick layers can be obtained by the use of large particles, but close packing of larger particles also results in lower density and therefore higher shrinkage during sintering than that of smaller particles. In a two step process a thick layer of a first EPD can be formed by large particles. The wide gaps between the large particles could be filled by a following second deposition of smaller particles (Fig. 8).

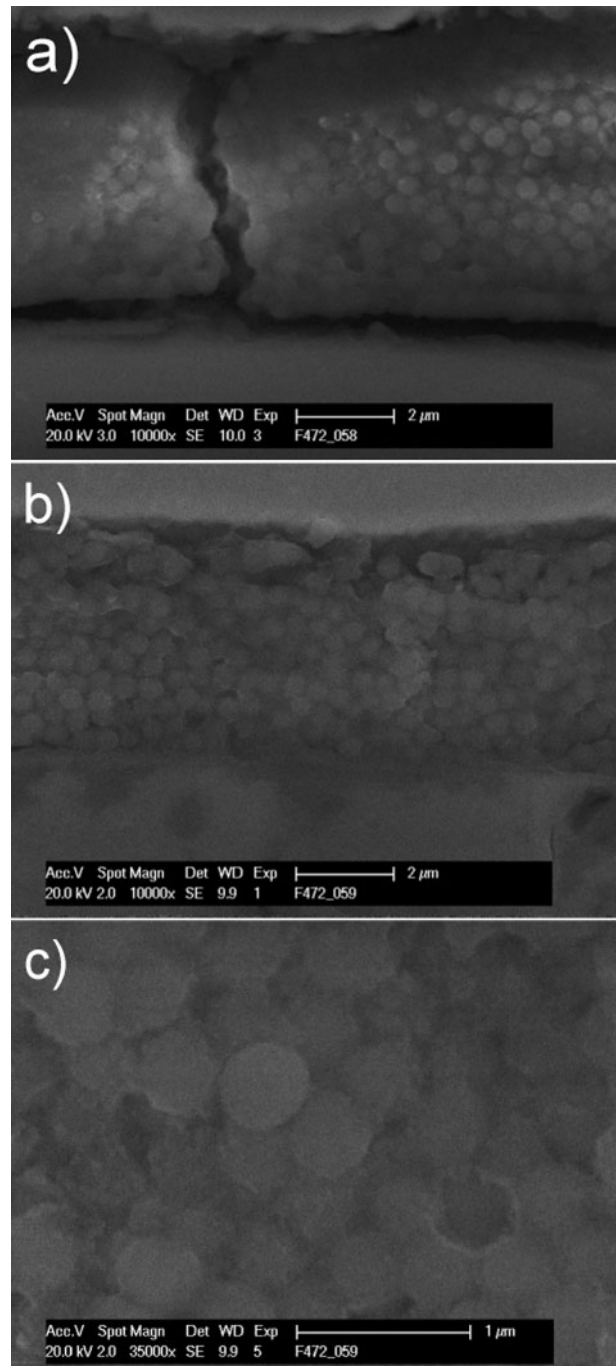


6 Electrochemical impedance spectroscopy spectra in 0.05M Na<sub>2</sub>SO<sub>4</sub> after 30 min immersion, 10<sup>2</sup>–10<sup>-1</sup> Hz, amplitude 10 mV: AZ31 uncoated (dashed), brush (dotted) and dip coated (solid); coating composition D6, sintered (400°C/2 h)



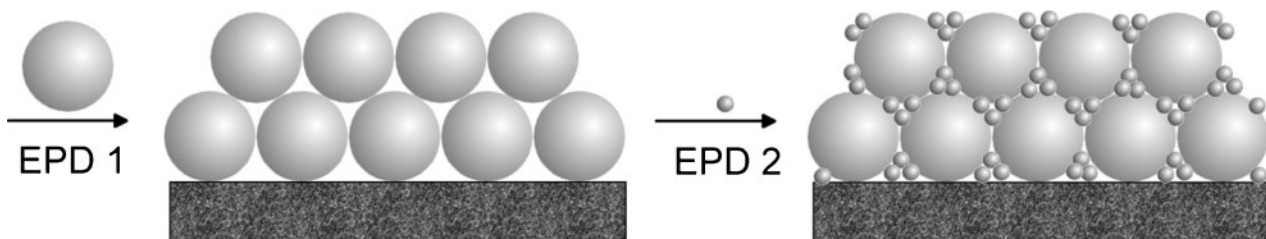
a 35 nm particles (80.1%SiO<sub>2</sub>, 13.8%B<sub>2</sub>O<sub>3</sub>, 6.1%P<sub>2</sub>O<sub>5</sub>; 2% in EtOH; 10 V/30 min); b 35 nm particles (80.1%SiO<sub>2</sub>, 13.8%B<sub>2</sub>O<sub>3</sub>, 6.1%P<sub>2</sub>O<sub>5</sub>; 1.0 wt-% PDES; 10 V/30 min); c 40 nm particles with boron rich surface and 0.5 wt-% PDES of same overall composition (10 V/30 min)

7 Images (SEM) of EPD layers on AZ31 sintered at 400°C for 2 h



a EPD with 400 nm particles (88.2%SiO<sub>2</sub>, 6.0%B<sub>2</sub>O<sub>3</sub>, 5.8%P<sub>2</sub>O<sub>5</sub>; 2% in EtOH, 3 V/5 min); b,c first EPD with 400 nm particles followed by second EPD with 10 nm particles (82.6%SiO<sub>2</sub>, 11.4%B<sub>2</sub>O<sub>3</sub>, 6.0%P<sub>2</sub>O<sub>5</sub>; 2% in EtOH; 6 V/30 min)

9 Images (SEM) of cross-sections on EPD layers on AZ31 sintered at 400°C for 2 h



8 Schematic drawing of two step coating process with first deposition of larger particles followed by second deposition of smaller particles

Thick layers of large particles (here with a diameter of 400 nm) crack during sintering and partly delaminate (Fig. 9a). If a second deposition of small particles (here 10 nm) is conducted immediately after the deposition of the large particles, up to 6 µm thick, crack free coatings can be obtained on AZ31 (Fig. 9b). Figure 9c shows the cross-section of this layer where a large particle has been ripped off during metallographic preparation. Apparently this particle was embedded in some kind of matrix probably consisting of the second, smaller particles. Therefore, it is evident that the gaps between the larger particles can readily be filled by the smaller ones. Thus thick, dense layers with small shrinkage and therefore no crack formation during sintering can be obtained.

## Conclusion

By dip coating, brushing and electrophoretic deposition thin transparent and crack free coatings based on nanoparticles could be applied onto the magnesium alloys AZ31 and AZ91. Sufficient densification of the coatings was already possible at moderate temperatures. Especially aluminium containing coatings show good properties after a heat treatment at 200°C, which should avoid any damaging of the magnesium substrate. However, the coating thickness, especially for dip coating and brushing is still quite low and should be increased to guarantee a good corrosion performance. Coating properties (mechanical stability, corrosion protection) are still under research. Further investigations should show if multilayer coatings or a combination of different methods could result in thicker coatings and therefore in a better corrosion protection.

Coatings based on commercially available nanoparticles have some advantages over coatings made from polymeric sols. The dispersions and additives to be used are less expensive than the alkoxides used in the classical sol-gel process. Hence the use of commercial products

further increases the value of this new method especially for industrial applications.

## Acknowledgement

This project has been funded by the German Ministry for Economics and Technology (BMWi) via the Arbeitsgemeinschaft industrieller Forschungsvereinigungen "Otto von Guericke" e.V. (AiF) with the number 14385 N.

## References

1. D. M. Liu: *J. Mater. Sci. Lett.*, 1998, **17**, 467–469.
2. H. Q. Nguyen, W. Fürbeth and M. Schütze: *Mater. Corros.*, 2002, **53**, 772–778.
3. W. Stöber, A. Fink and E. Bohn: *J. Colloid Interf. Sci.*, 1968, **26**, 62–69.
4. M. D'Apuzzo, A. Aronne, S. Esposito and P. Pernice: *J. Sol-Gel Sci. Tech.*, 2000, **17**, 247–254.
5. J. D. Soraru, F. Babonneau, C. Gervais and N. Dallabona: *J. Sol-Gel Sci. Tech.*, 2000, **18**, 11–19.
6. M. Prassas and L. L. Hench: in 'Ultrastructure processing of ceramics, glasses & composites', (ed. L. L. Hench and D. R. Ulrich), 100–125; 1984, New York, Wiley.
7. M. A. Villegas and J. M. Fernandez Navarro: *J. Mater. Sci.*, 1988, **23**, 2464–2478.
8. C. J. Brinker and G. Scherer: 'Sol-Gel science'; 1989, New York, Academic Press.
9. C. J. Brinker, G. C. Frye, A. J. Hurd and C. S. Ashley: *Thin Solid Films*, 1991, **201**, 97–108.
10. M. M. Collinson, N. Moore, P. N. Deepa and M. Kanungo: *Langmuir*, 2003, **19**, 7669–7672.
11. H. Schmidt, G. Jonschker, S. Goedicke and M. Menning: *J. Sol-Gel Sci. Tech.*, 2000, **19**, 39–51.
12. J. Gallardo, P. Galliano, R. Moreno and A. Duran: *J. Sol-Gel Sci. Tech.*, 2000, **19**, 107–111.
13. H. Scholze: 'Glas: Natur, Struktur und Eigenschaften'; 1988, Berlin, Springer-Verlag.
14. H. C. Hamaker and E. J. W. Verwey: *Trans. Faraday Soc.*, 1940, **36**, 180–185.
15. Z. S. Rak: *cfilBer. DKG*, 2000, **77**, 6–16.
16. L. Besra and M. Liu: *Prog. Mater. Sci.*, 2007, **52**, 1–61.
17. R. N. Basu, C. A. Randall and M. J. Mayo: *J. Am. Ceram. Soc.*, 2001, **84**, 33–40.